Available online at www.sciencedirect.com
SCIENCE DIRECT
Biochemical and Biophysical Research Communications 343 (2006) 49–56
BBRC
www.elsevier.com/locate/ybbrc

Binding of IRBIT to the IP_3 receptor: Determinants and functional effects

Benoit Devogelaere [a], Nael Nadif Kasri [a], Rita Derua [b], Etienne Waelkens [b], Geert Callewaert [a], Ludwig Missiaen [a], Jan B. Parys [a], Humbert De Smedt [a,*]

[a] *Laboratorium voor Fysiologie, Katholieke Universiteit Leuven Campus Gasthuisberg O/N1, Leuven, Belgium*
[b] *Laboratorium voor Biochemie, Katholieke Universiteit Leuven Campus Gasthuisberg O/N1, Leuven, Belgium*

Received 20 February 2006
Available online 28 February 2006

Abstract

IRBIT has previously been shown to interact with the inositol 1,4,5-trisphosphate (IP_3) receptor (IP_3R) in an IP_3-sensitive way. So far it remained to be elucidated whether this interaction was direct or indirect, and whether it was functionally relevant. We now show that IRBIT can directly interact with the IP_3R, and that both the suppressor domain and the IP_3-binding core of the IP_3R are essential for a strong interaction. Moreover, we identified a PEST motif and a PDZ-ligand on IRBIT which were critical for the interaction with the IP_3R. Furthermore, we identified Asp-73 as a critical residue for this interaction. Finally, we demonstrated that this interaction functionally affects the IP_3R: IRBIT inhibits both IP_3 binding and IP_3-induced Ca^{2+} release.

Keywords: IRBIT; PEST motif; PDZ-ligand; Inositol 1,4,5-trisphosphate receptor; IP_3-induced Ca^{2+} release; Point-mutation

The inositol 1,4,5-trisphosphate (IP_3) receptor (IP_3R) is a key component for intracellular Ca^{2+} signalling. IP_3Rs are tetrameric intracellular Ca^{2+}-release channels [1] encoded by three different genes [2]. The IP_3R structure consists of three distinct regions: an N-terminal ligand-binding domain (lbd), an internal coupling domain, and a C-terminal channel domain [2,3]. The lbd, which stretches from amino acid (aa) 1 to 604, can be subdivided into a suppressor domain and an IP_3-binding core. The latter is necessary and sufficient for high-affinity binding of IP_3 [4].

To control an extensive array of functions, Ca^{2+} signals are accurately regulated in space, time, and amplitude [5,6]. The complex regulation of Ca^{2+} signals has been partly attributed to the diversity of IP_3R isoform expression, assembly of heterotetrameric IP_3R complexes, subcellular distribution of the IP_3R, and regulation of the IP_3R by many cellular regulators such as Ca^{2+}, ATP, phosphatidylinositol 4,5-bisphosphate (PIP_2), thiol-reactive agents, and phosphorylation [2,7–10]. The IP_3R is also regulated by a vast number of interacting proteins, including calmodulin, CaBP1, kinases, phosphatases, and components of the cytoskeleton [11].

Recently, a new protein that interacts with the IP_3R in an IP_3-sensitive way was discovered: IRBIT, the IP_3R-binding protein released by inositol 1,4,5-trisphosphate [12]. The cDNA encoding IRBIT was discovered by Dekker et al. [13]. The corresponding protein was shown to interact with the IP_3R, though it was not demonstrated whether this interaction was direct or indirect [12]. Moreover, the functional relevance of the interaction IRBIT-IP_3R remained unclear.

In this study, we demonstrated that IRBIT directly interacted with the IP_3R and that this interaction was dependent on two specific motifs on IRBIT: a PEST motif and a PDZ-ligand. Moreover, we showed that this interaction affected the functioning of the IP_3R: both IP_3 binding and IP_3-induced Ca^{2+} release (IICR) were inhibited by submicromolar concentrations of IRBIT.

Materials and methods

Materials. IP_3, PIP_2 from brain extract and bovine serum albumin (BSA) were obtained from Sigma-Aldrich NV (Bornem, Belgium).

* Corresponding author. Fax: +32 16 34 59 91.
E-mail address: Humbert.Desmedt@med.kuleuven.be (H. De Smedt).

0006-291X/$ - see front matter © 2006 Elsevier Inc. All rights reserved.
doi:10.1016/j.bbrc.2006.02.119

Glutathione Sepharose 4B, $^{45}Ca^{2+}$, Enhanced Chemiluminescence (ECL) Plus, and HyperFilm were from Amersham Biosciences Europe GmbH (Freiburg, Germany). *Strep*-Tactin® Superflow®, *Strep*-Tactin HRP conjugate, and pEXPR-IBA103 were from IBA GmbH (Göttingen, Germany). Complete™ Protease Inhibitors and alkaline phosphatase from calf intestine were from Roche Diagnostics GmbH (Penzberg, Germany). pFASTBAC™1, Sypro® Orange, NuPAGE® gels, MOPS buffer, Sf9 cells, and all cell culture media and supplements were from Invitrogen Ltd (Paisley, UK). GeneJuice Transfection Reagent and pET21b were from EMD Biosciences Inc (Madison, WI). Slide-A-Lyzer and Profound Pull-Down Glutathione *S*-transferase (GST) protein–protein interaction kit were from Pierce Biotechnology Inc. (Rockford, IL).

Cell culture. COS-1, HeLa, and Sf9 cells were cultured as described previously [10,14,15]. L15 cells were obtained by stable exogenous expression of IP_3R1 in Lvec cells, whereas Lvec cells represent the control cells expressing the empty vector [16]. These cells, initially a gift from Dr. K. Mikoshiba (University of Tokyo, Japan), were cultured as described previously [15].

Plasmid vectors and baculovirus construction. Mouse IRBIT cDNA (clone 4007102) was obtained from the I.M.A.G.E. Consortium (Livermore, CA). The cDNA fragments corresponding to aa 1–530, 1–520, and 1–64 of mouse IRBIT were cloned into the eukaryotic OneSTrEP fusion vector pEXPR-IBA103 to generate the OneSTrEP-tagged IRBIT, IRBIT[ΔPDZ], and IRBIT[1–64] constructs, respectively. The cDNA fragments corresponding to aa 93–530 and 93–520 were subcloned into pEXPR-IBA103-IRBIT[1–64], resulting in, respectively, IRBIT[ΔPEST] and IRBIT[ΔPEST, ΔPDZ].

The deletion mutants IRBIT[Δ70-73] and IRBIT[Δ82-88], in which the peptides 70-SSTD-73 and 82-TDSSDDE-88 were, respectively, deleted, were generated via PCR-mediated overlap extension and were also cloned into pEXPR-IBA103. The point-mutants IRBIT[D73R] and IRBIT[D-DE88KKK], in which residue Asp-73 and peptide 86-DDE-88 were replaced by Arg and the peptide KKK, respectively, were also generated via PCR-mediated overlap extension and cloned into pEXPR-IBA103. The IRBIT and IRBIT[ΔPEST] fragments were subcloned into pEGFP-C2 to enable expression of GFP-fusion proteins. All constructs were sequenced using the MegaBACE 500 DNA sequencing System (Amersham Biosciences Europe GmbH).

The *Eco*RI/*Hin*dIII fragment of pEXPR-IBA103-IRBIT was subcloned into the pET21b vector to enable expression of OneSTrEP-tagged IRBIT in bacteria. The same fragment was subcloned into pFASTBAC™1, resulting in pFASTBAC™1-IRBIT-OneSTrEP. The latter was used to generate the recombinant IRBIT-OneSTrEP baculovirus according to the manufacturer's protocols (Bac-to-Bac® Baculovirus Expression System, Invitrogen Ltd).

Transfections and infections. Mammalian cells were plated and transfected with GeneJuice Transfection Reagent as described in the manufacturer's protocol. Sf9 insect cells were infected with a high-titer viral stock of the recombinant baculovirus at 1×10^8 pfu/ml. All cells were harvested and/or analyzed 48 h after transfection/infection.

Preparation of cleared Escherichia coli lysates and purification of GST-fusion proteins. For preparation of GST-fusion proteins, pGEX6p2 constructs containing the coding sequence for aa 1–225, 226–604, and 1–604 of mouse IP_3R1 [10] were transformed into BL21 *E. coli*. Colonies were grown overnight in 50 ml of Luria-Bertani medium at 37 °C. Luria-Bertani medium (400 ml) was added to this preculture, and bacteria were further grown at 28 °C until A_{600} amounted to 0.8. Protein expression was induced by adding 0.1 mM isopropyl-thio-β-D-galactopyranoside to the bacterial culture, which was further grown at 14 °C for another 20 h. Bacterial cells were harvested and lysed by sonication. Lysates were cleared via centrifugation (10,000*g*, 10 min) at 4 °C. This procedure was also performed to obtain cleared lysates from *E. coli* cells expressing IRBIT-OneSTrEP. The soluble fractions were incubated for 2 h with Glutathione Sepharose 4B beads. After washing the beads, GST-fusion proteins were eluted with glutathione as described previously [17]. Purified proteins were dialyzed overnight against phosphate-buffered saline (PBS), using Slide-A-Lyzer with a cut-off of 10 kDa and stored at −80 °C.

Preparation of cleared lysates from COS-1 and Sf9 cells. Cells were collected and lysed in RIPA buffer (25 mM Hepes, 0.3 mM NaCl, 1.5 mM $MgCl_2$, 0.5 mM DTT, 20 mM β-glycerolphosphate, 10% (v/v) glycerol, 1 mM Na_3VO_4, and 1% (v/v) Triton X-100, pH 7.5) supplemented with Complete™ protease inhibitors. The lysates were cleared via centrifugation (10,000*g*, 10 min) at 4 °C. Dephosphorylation was obtained by incubating the cleared lysates with or without 0.4 i.u./μl alkaline phosphatase in the presence of phosphatase buffer for 10 min at 37 °C after which 20 mM EGTA, pH 7.4, was added.

Purification of IRBIT-OneSTrEP from cleared lysates. Cleared lysates from COS-1, Sf9 or *E. coli* cells were incubated with *Strep*-Tactin matrix at 4 °C for 30 min in a head-over-head rotator. The matrix was washed five times with high-salt wash buffer (100 mM Tris–HCl, 500 mM NaCl, 250 mM $(NH_4)_2SO_4$, 100 mM $MgCl_2$, 1 mM EDTA, and 0.20% (v/v) Tween 20 at pH 8.0). IRBIT was eluted with desthiobiotin elution buffer (5 mM D-desthiobiotin, 100 mM Tris–HCl, 150 mM NaCl, and 1 mM EDTA, pH 8.0). Purity of the protein was confirmed with SDS–PAGE followed by Sypro® Orange protein gel staining and quantification was done using a BSA-standard.

GST pull-down assay. GST pull-down assays were performed by using the Profound Pull-Down GST protein–protein interaction kit. Purified and dialyzed GST-IP_3R1 fusion proteins or parental GST (control) were incubated with purified IRBIT or IRBIT-containing, cleared lysate in pull-down buffer (50 mM Tris–HCl and 1 mM EGTA at pH 7.4, unless stated) and immobilized on Glutathione Sepharose 4B beads via rotation in a head-over-head rotator for 1 h at 4 °C. IP_3 and PIP_2 were dissolved in pull-down buffer and added prior to this incubation. For experiments involving PIP_2, incubations were performed at 30 °C to ensure its full dissolution. The beads were washed 4 times with pull-down buffer and the GST-IP_3R1/IRBIT complex was eluted with 100 mM glutathione in pull-down buffer. Eluates were further analyzed by SDS–PAGE as described. Presence of the GST-fusion proteins in the eluates was confirmed by Sypro® Orange protein gel staining prior to electroblotting (data not shown).

SDS–PAGE and downstream analysis. Protein samples were analyzed by NuPAGE® 4–12% (v/v) Bis–Tris SDS/polyacrylamide gels using MOPS buffer. Total protein content was visualized with Sypro® Orange protein gel staining and a Storm840 FluorImager (Amersham Biosciences Europe GmbH). After semi-dry electroblotting onto a PVDF membrane (Immobilon-P; Millipore, Bedford, MA) and blocking with PBS containing 0.5% (v/v) Tween 20 and 5% (w/v) BSA, the blots were incubated with the HRP-conjugated *Strep*-Tactin monoclonal antibody. The immunoreactive bands were visualized with ECL Plus substrate and exposed to HyperFilm. The HyperFilm was developed using a KODAK X-Omat 1000 (KODAK, Rochester, NY) and quantification was done with TotalLab software (Non-linear Dynamics, Newcastle-upon-Tyne, UK).

Microsequencing. IRBIT-OneSTrEP was purified from a cleared lysate of transfected COS-1 cells. Samples were essentially analyzed as described previously [18]. Briefly, proteins were separated by SDS–PAGE on 10% polyacrylamide gels and electroblotted onto a ProBlot PVDF membrane (Applied Biosystems) in 10 mM 3-cyclohexylamino-1-propanesulfonic acid, 10% (v/v) methanol at pH 11.0. The membrane was subsequently stained for 30 s in 0.1% (w/v) Amido Black. The protein bands of interest were cut out and analyzed by a 492 Procise (Applied Biosystems, Foster City, CA) amino acid sequencer based on Edman degradation chemistry.

[^{3}H]IP_3 binding. Measurements were performed as described previously [19]. Essentially [^{3}H]IP_3 binding was performed at 0 °C by incubating 1.5 μg purified GST-IP_3R1[1–604] with 1.5 nM [^{3}H]IP_3 (Perkin-Elmer; Boston, MA) and varying amounts of unlabelled IP_3 or purified IRBIT from Sf9 cells in 100 μl of IP_3-binding buffer (50 mM Tris–HCl, 1 mM EDTA, and 10 mM 2-mercaptoethanol, pH 7.4). After 30 min of incubation, 10 μl of γ-globulin (20 mg/ml) and 110 μl of 20% (w/v) polyethylene glycol in IP_3-binding buffer were added and the samples were rapidly filtered through glass-fiber filters. Non-specific binding was determined in the presence of 12.5 μM unlabelled IP_3.

$^{45}Ca^{2+}$-flux assays. $^{45}Ca^{2+}$ fluxes were performed on saponin-permeabilized L15 and Lvec cells [16] in essentially the same way as described previously [15]. Briefly, the cells were grown in 12-well clusters (Costar,

MA) until confluent. Cells were permeabilized and the non-mitochondrial Ca^{2+} stores were loaded with $^{45}Ca^{2+}$ (23 μCi/ml). The cells were washed twice with 1 ml of efflux medium containing 10 μM thapsigargin to block the endoplasmic reticulum (ER) Ca^{2+} pumps. The efflux medium was replaced every 2 min. Purified IRBIT from Sf9 cells was added to a total concentration of 250 nM 2 min prior to IP_3 addition. At the end of the experiment, the $^{45}Ca^{2+}$ remaining in the stores was released by incubation with 1 ml of a 2% (w/v) SDS solution for 30 min. Ca^{2+} release was determined as the fractional loss and normalized to the total releasable fraction by 5 μM A23187, which was taken as 100%.

Results

A direct interaction between IRBIT and the lbd of IP_3R1

To investigate whether IRBIT directly interacted with the lbd of IP_3R1, the mouse cDNA of IRBIT was cloned into the OneSTrEP tag fusion vector pEXPR-IBA103. Using the affinity of the OneSTrEP tag to the *Strep*-Tactin matrix, IRBIT was purified from COS-1 cells. Potentially interacting proteins were completely removed by extensive washing with a high-salt buffer. The purified IRBIT protein was detected as a strong band with a molecular mass of approximately 63 kDa by Sypro® Orange protein gel staining (Fig. 1A), which is in agreement with the calculated mass of recombinant IRBIT-OneSTrEP. In the same purified IRBIT sample, a 55 kDa protein, also reactive against the highly specific *Strep*-Tactin antibody, was present (Figs. 1A and B, lane 1). The N-terminal aa stretch of this protein was determined by microsequencing as SYSSAAS, which corresponds to IRBIT aa 74–80. We concluded that the 55 kDa protein corresponded to C-terminally One-STrEP-tagged, N-terminally truncated IRBIT[74–530], which was in agreement with the observed mass.

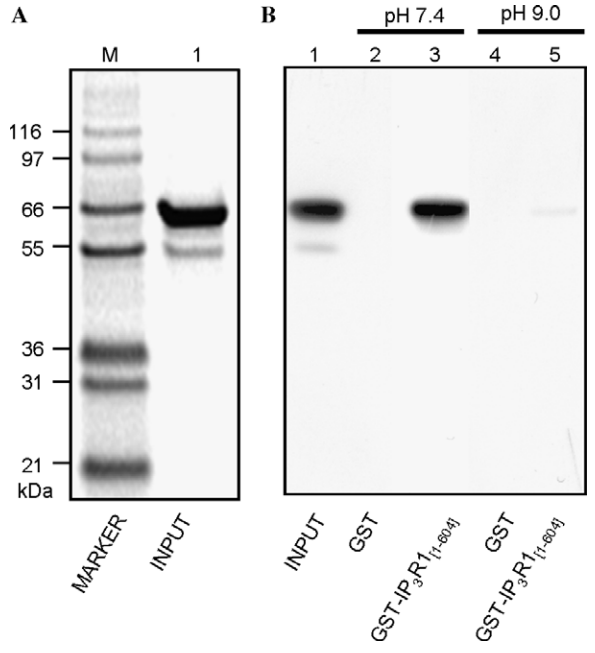

Fig. 1. IRBIT purified from COS-1 cells binds directly to the lbd of IP_3R1 at a physiological pH. (A) Recombinant IRBIT was purified from COS-1 cells using the affinity of the OneSTrEP tag to the *Strep*-Tactin matrix. Additional washings with high-salt wash buffer were included to completely remove interacting proteins. Purity of the sample was determined by SDS–PAGE followed by Sypro® Orange total protein gel staining (lane 1). Mark12™ Unstained Standard (Invitrogen) was used as molecular weight reference (M). (B) Purified IRBIT (lane 1) was incubated with Glutathione Sepharose and GST or GST-IP_3R1[1–604] in pull-down buffer at pH 7.4 (lanes 2 and 3) or pH 9.0 (lanes 4 and 5). Incubates were washed, eluted with glutathione, and analyzed with SDS–PAGE and Western blotting. Amount of sample used in lanes 2–5 was 2-fold higher as compared to lane 1. Results were typical for at least three experiments.

Purified IRBIT was then subjected to a pull-down assay with GST-IP_3R1[1–604] in a pull-down buffer at pH 7.4. After elution, the sample was processed by SDS–PAGE. IRBIT was visualized by chemiluminescent detection using the *Strep*-Tactin monoclonal antibody. In this condition, up to 50% of the IRBIT input remained bound to GST-IP_3R1[1–604] and the interaction was specific, as IRBIT did not interact with the parental GST protein (Fig. 1B, lanes 2 and 3). Interestingly, the IRBIT[74–530] fragment was not withheld in the pull-down assay (Fig. 1B, lane 3).

We investigated whether the in vitro binding characteristics of IRBIT and IP_3 corresponded with respect to pH-dependence. Therefore, the pH of the pull-down buffer was raised to pH 9.0, which should allow optimal IP_3 binding [20]. Under these conditions, the amount of IRBIT bound to GST-IP_3R1[1–604] was reduced to only a few percents of the binding observed at pH 7.4 (Fig. 1B, lanes 4 and 5).

To investigate the relevance of the cellular source of IRBIT, the cDNA encoding IRBIT-OneSTrEP was subcloned into the bacterial expression vector pET21b. In addition, a recombinant baculovirus was made for expression of IRBIT-OneSTrEP in Sf9 insect cells. IRBIT was purified from both cellular sources and subjected to the pull-down assay with GST-IP_3R1[1–604] at pH 7.4. IRBIT derived from insect cells, but not from bacterial cells, could be specifically retained and recovered in the eluates (data not shown). The inability of IRBIT derived from bacteria to interact with GST-IP_3R1[1–604] could be due to its improper phosphorylation. Indeed, the interaction between IRBIT and GST-IP_3R1[1–604] was abolished by alkaline phosphatase treatment (data not shown), which is in agreement with previous findings [12].

A strong interaction between IRBIT and IP_3R1 is highly dependent on a PEST motif and a PDZ-ligand on IRBIT, as well as on both the suppressor domain and the IP_3-binding core of IP_3R1

Via an in silico search for protein domains on IRBIT using the Pfam database (http://pfam.wustl.edu/), a PEST motif and a class-II PDZ-ligand were found on IRBIT (Fig. 2A). The PEST motif stretches from residue 65 to 92 and is thus disrupted by the observed proteolysis between aa 73 and 74 which abolished binding to IP_3R1[1–604] (Fig. 1B, lane 3). The PDZ-ligand corresponds to the very C-terminus of IRBIT, from aa 520 to 530 with Tyr–Tyr–Arg–Tyr–COOH as core sequence.

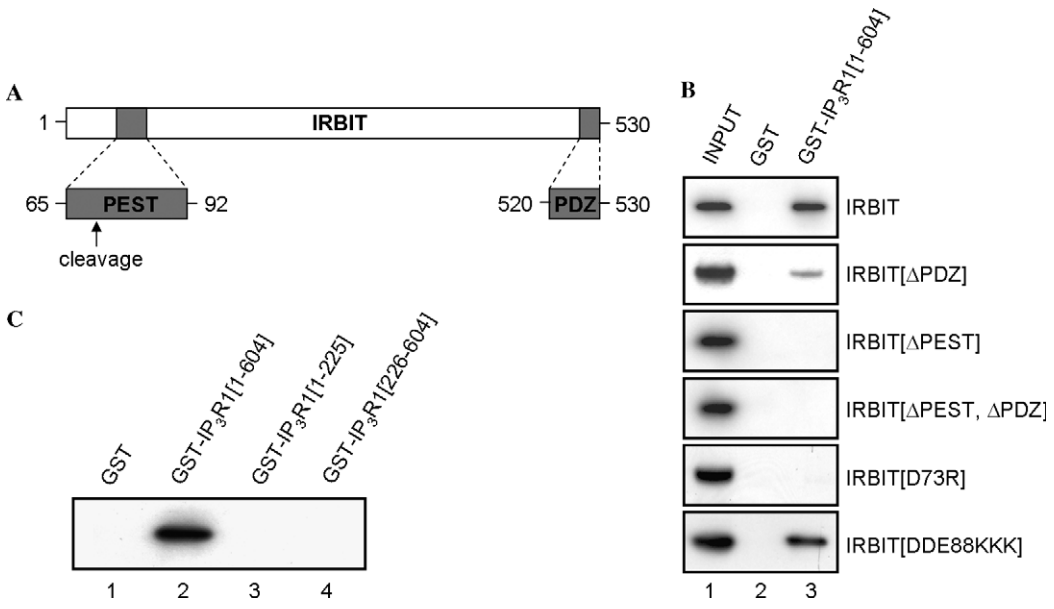

Fig. 2. The complex interaction between IRBIT and the IP_3R is dependent on a PEST motif and PDZ-ligand on IRBIT, and the suppressor domain and IP_3-binding core on the IP_3R. (A) IRBIT contains two domains that interact with IP_3R1[1–604] : a PEST motif (PEST) from aa 65 to 92 and a PDZ-ligand (PDZ) from aa 520 to 530. These motifs were found via an in silico search using the Pfam database (http://pfam.wustl.edu/). The in vivo cleavage site between aa 73 and 74 was found by microsequencing. (B) The cleared COS-1 lysates containing IRBIT, IRBIT[ΔPDZ], IRBIT[ΔPEST], IRBIT[ΔPEST, ΔPDZ], IRBIT[D73R], and IRBIT[DDE88KKK] (lane 1) were subjected to a pull-down with GST (lane 2) or GST-IP_3R1[1–604] (lane 3). Incubates were washed, eluted with glutathione, and analyzed with SDS–PAGE and Western blotting. Amount of sample used in lanes 2 and 3 was 5-fold higher as compared to lane 1. (C) Cleared COS-1 lysate containing IRBIT was subjected to a pull-down with GST-IP_3R1[1–604] (lane 2), GST-IP_3R1[1–225] (lane 3), GST-IP_3R1[226-604] (lane 4) or GST (parental control, lane 1). Incubates were washed, eluted with glutathione, and analyzed using SDS–PAGE and Western blotting. All results were typical for at least three experiments.

To investigate the relevance of these motifs for the interaction with IP_3R1, the corresponding deletion constructs were cloned into pEXPR-IBA103. These constructs enabled expression of IRBIT[ΔPEST], IRBIT[ΔPDZ], and the double mutant IRBIT[ΔPEST, ΔPDZ] in COS-1 cells. The cleared lysates from the various mutants were subjected to a pull-down assay and the eluates were analyzed (Fig. 2B). IRBIT[ΔPDZ] could interact with GST-IP_3R1[1–604], though the interaction was approximately halved compared to wild-type IRBIT. IRBIT[ΔPEST] on the other hand could not be detected in the eluates, indicating that the interaction was too weak. The same was true for the double mutant IRBIT[ΔPDZ, ΔPEST] which was also undetectable in the eluates. This indicates that the presence of the PEST motif is essential for the interaction with the lbd of IP_3R, and that the PDZ-ligand is required for maximal affinity.

We reasoned that negatively charged (Asp, Glu) or putatively phosphorylated (Ser, Thr, and Tyr) residues in the PEST motif could be important for the interaction between IRBIT and the lbd of IP_3R1. As the peptides 70–73 and 82–88 of IRBIT are rich in such residues, the corresponding deletion mutants IRBIT[Δ70–73] and IRBIT[Δ82–88] were generated. Neither of the two deletion mutants could be detected in the eluates, indicating that the corresponding deletions disabled interaction with the lbd of IP_3R1 (data not shown). In addition, the point-mutants IRBIT[D73R] and IRBIT[DDE88KKK] were generated (see Materials and methods). These mutants were analyzed via the pull-down assay with GST-IP_3R1[1–604], as shown in Fig. 2B. Interestingly, the specific point-mutation at position 73 was sufficient to disrupt the interaction. IRBIT[DDE88KKK] in contrast interacted comparably to wild-type IRBIT. This points again to the relevance of the PEST motif as a main interaction site for the IP_3R and indicates a crucial role for Asp-73. It is noteworthy that the observed in vivo cleavage right after this residue also forms an IRBIT protein unable to interact with the IP_3R.

We further confirmed the relevance of the PEST motif by comparing the subcellular localization of the GFP-fusion proteins GFP-IRBIT and GFP-IRBIT[ΔPEST]. We found that wild-type IRBIT extensively colocalized with the ER. IRBIT[ΔPEST] in contrast showed a clear nuclear localization and did not colocalize with the ER (data not shown).

The lbd of the IP_3R is known to consist of two distinct domains: the suppressor domain (aa 1–225) and the IP_3-binding core (aa 226–604). To investigate the relevance of these two subdomains for the interaction with IRBIT, a pull-down assay was performed with GST-IP_3R1[1–225] and GST-IP_3R1[226–604] [10]. IRBIT could be detected in the eluates of the complete lbd GST-IP_3R1[1–604], but neither in the eluates of the suppressor domain GST-IP_3R1[1–225] nor of the IP_3-binding core GST-IP_3R1[226–604] (Fig. 2C). This finding illustrates the

importance of the complete lbd for a strong interaction with IRBIT but might look contradictory with previous findings where the interaction of endogenous IRBIT with the IP_3-binding core alone was shown [12]. However, using 10-fold longer exposure times we could confirm a weak interaction with the IP_3-binding core alone (data not shown). This indicates that IRBIT could interact weakly with the IP_3-binding core alone, but that the suppressor domain is additionally required to establish a strong interaction with IRBIT.

The PDZ-ligand of IRBIT mediates an IP_3-insensitive interaction with the IP_3R

IRBIT was identified as a protein interacting with the IP_3R in an IP_3-sensitive way [12]. Therefore, the effects of IP_3 on the in vitro interaction between IRBIT present in a cleared COS-1 lysate and the GST-IP_3R1[1–604] were examined via a pull-down assay to measure the strength of the interaction. The relative amount of IRBIT bound to the IP_3R was quantified and plotted as a function of the IP_3 concentration. IP_3 could dissociate IRBIT from GST-IP_3R1[1–604] in a dose-dependent manner (Fig. 3). However, even at a high concentration of IP_3 (100 μM), approximately 30% of the IRBIT input remained bound and thus appeared IP_3-insensitive. Half-maximal competition was achieved around 14 μM IP_3. Interestingly, we found that PIP_2 also disrupted the interaction between IRBIT and the IP_3R in a similar way as IP_3 (data not shown).

To elucidate a possible role of the PDZ-ligand in the IP_3-insensitive binding, the interaction between GST-IP_3R1[1–604] and IRBIT[ΔPDZ] was assayed as a function of the IP_3 concentration (Fig. 3). In contrast to wild-type IRBIT, IP_3 could completely disrupt the interaction with IRBIT[ΔPDZ] with an IC_{50} of approximately 10 μM. This shows that the PDZ-ligand is responsible for an IP_3-insensitive interaction with the IP_3R, which constitutes hence a new aspect of the IRBIT-binding to the IP_3R.

IRBIT functionally affects the IP_3R1: IRBIT inhibits IP_3 binding and IICR

To investigate whether the interaction between IRBIT and the IP_3R was functionally relevant, we examined whether IRBIT could disrupt the binding of IP_3 to the IP_3R. A [^{3}H]IP_3-binding assay was performed with purified GST-IP_3R1[1–604] in the presence of increasing concentrations of unlabelled IP_3 (Fig. 4, triangles) or IRBIT purified from Sf9 cells (Fig. 4, squares). In this condition, IP_3 and IRBIT completely inhibited [^{3}H]IP_3binding to GST-IP_3R1[1–604] with an IC_{50} of 26 ± 3 and 250 ± 20 nM, respectively, as determined by a logistic fit (Origin, OriginLab Corporation, Northampton, UK). This indicates that under these conditions the apparent affinity of IRBIT is approximately 10-fold lower compared to that of IP_3.

As IRBIT clearly competed with IP_3 for binding to GST-IP_3R1[1–604], we examined the effect of IRBIT on IICR in L15 cells, which predominantly express IP_3R1. Addition of 0.5 μM IP_3 induced $^{45}Ca^{2+}$ release from the non-mitochondrial intracellular stores. This Ca^{2+} release was strongly inhibited by 250 nM IRBIT (Fig. 5). IRBIT (250 nM) increased the EC_{50} for IICR from 0.39 ± 0.05 μM to 2.31 ± 0.68 μM IP_3 (Fig. 5). Similar results were obtained with Lvec cells, which predominantly

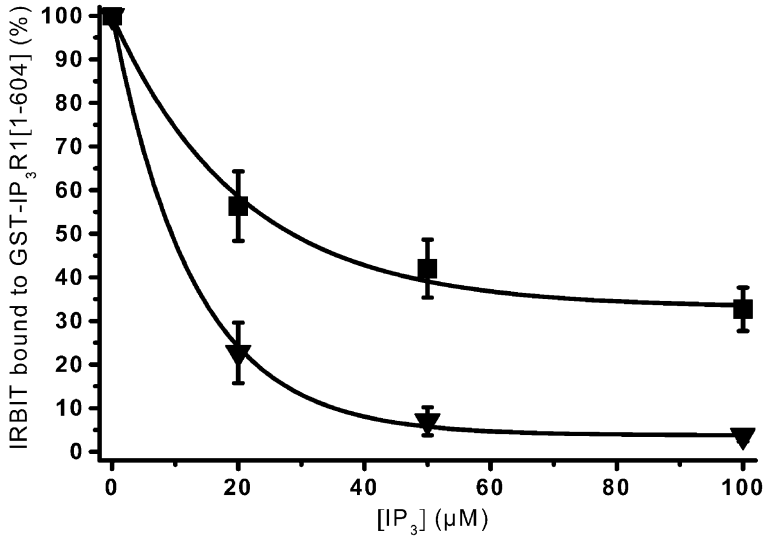

Fig. 3. The PDZ-ligand mediates an IP_3-insensitive interaction with IP_3R1. The cleared COS-1 lysates containing IRBIT (squares) or IRBIT[ΔPDZ] (triangles) were subjected to a pull-down with GST-IP_3R1[1–604] in the presence of different concentrations of IP_3. Incubates were washed, eluted with glutathione, and analyzed using SDS–PAGE and Western blotting. The relative amount of IRBIT bound to GST-IP_3R1[1–604] was quantified using the TotalLab software (Non-linear Dynamics) and data are expressed as means ± SE of three independent experiments.

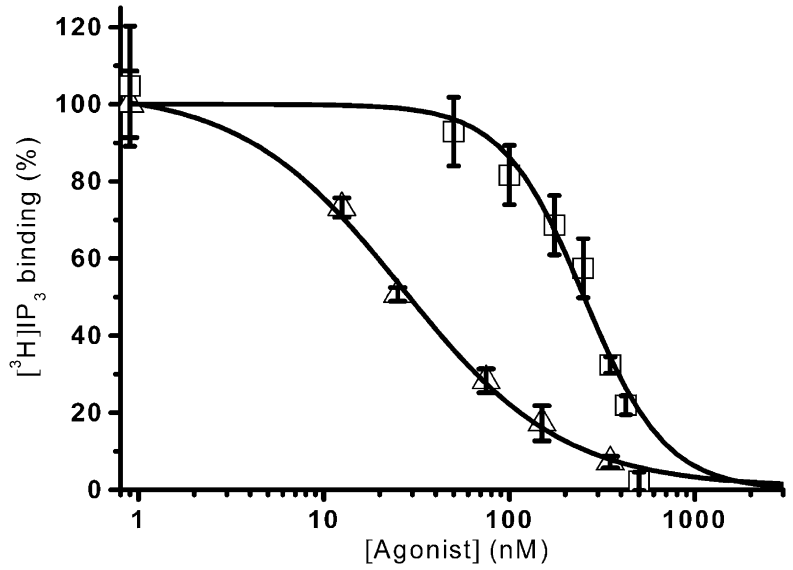

Fig. 4. IRBIT disrupts the binding of [^{3}H]IP$_3$ to IP$_3$R1. [^{3}H]IP$_3$ binding to 1.5 μg purified GST-IP$_3$R1[1–604] as a function of the concentration of unlabelled IP$_3$ (triangles) or IRBIT purified from Sf9 insect cells (squares). Binding was measured at pH 7.4 in the presence of 1 mM EDTA and 1.5 nM [^{3}H]IP$_3$. Data are expressed as means ± SE of at least five independent experiments.

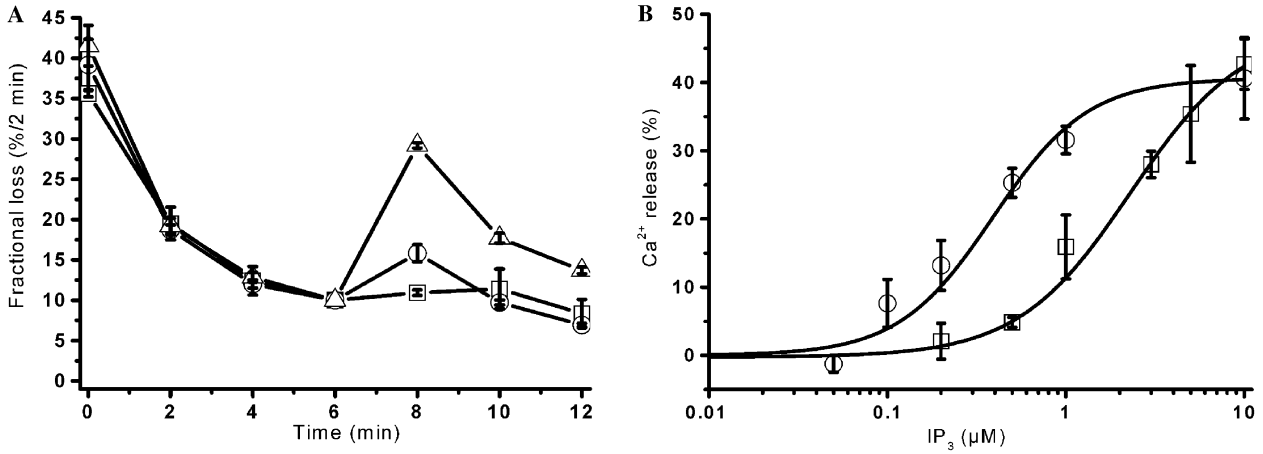

Fig. 5. IRBIT inhibits the IICR in permeabilized L15 fibroblasts. (A) $^{45}Ca^{2+}$-flux assay was performed on saponin-permeabilized L15 cells stimulated with 0.5 μM IP$_3$ in the absence (circles) or presence (squares) of 250 nM IRBIT purified from Sf9 cells. $^{45}Ca^{2+}$ release was plotted as the fractional loss during 2 min. $^{45}Ca^{2+}$ release by addition of 5 μM of A23187 was used as a reference (triangles). Each point is the mean ± SE of at least three independent experiments. (B) $^{45}Ca^{2+}$-flux assay was performed on saponin-permeabilized L15 cells with varying concentrations of IP$_3$ in the absence (circles) or presence (squares) of 250 nM IRBIT purified from Sf9 cells. Data values were normalized to the A23187-induced Ca^{2+} release, which was taken as 100%. Each point is the mean ± SE of at least three independent experiments.

express IP$_3$R3 (data not shown), showing that the interaction between IRBIT and the IP$_3$R is functionally relevant.

Discussion

The IRBIT protein was described by Ando et al. [12] as an IP$_3$R-binding protein released from the IP$_3$R upon addition of IP$_3$, but the existence of a direct interaction or the functional effects of the interaction remained unclear.

Using purified recombinant IRBIT, we showed that IRBIT could directly bind to the lbd of the IP$_3$R1 in the absence of other putative interacting proteins. IRBIT interacted strongly at a physiological pH of 7.4 but only very weakly at the more alkaline pH of 9.0. This is in contrast to the in vitro binding characteristics of IP$_3$ [20] and indicates that the molecular determinants of the binding sites might be different. IRBIT disrupted the binding of [^{3}H]IP$_3$ to the lbd of IP$_3$R1 with an apparent 10-fold lower affinity compared to unlabelled IP$_3$. Yet, at high concentrations IRBIT could completely disrupt the binding of [^{3}H]IP$_3$. This contrasts with the inability of IP$_3$ to completely disrupt the binding of IRBIT to the lbd of IP$_3$R1. This suggests that IRBIT and IP$_3$ share at least one common binding site on the lbd of IP$_3$R1, but also that IRBIT binds to at least

one site that is not common with the IP_3-binding pocket and that might be located on the suppressor domain. Previous experiments showed that the IP_3-binding core was sufficient for binding endogenous IRBIT [12], but we demonstrated that the suppressor domain is additionally required for establishing a strong interaction with recombinant IRBIT. Although the crystal structure of IRBIT in complex with the IP_3R remains to be determined, our data already suggested that IRBIT may have multiple interaction sites located on both the suppressor domain and the IP_3-binding core.

An in silico analysis revealed the presence of a PEST motif in the N-terminal region of IRBIT (aa 65–92) and a class-II PDZ-ligand in the very C-terminus (aa 520–530; see Fig. 2A). PEST motifs are polypeptide sequences enriched in Pro, Glu, Ser, and Thr that target proteins for rapid proteolytic degradation [21]. We identified an in vivo cleavage site inside this PEST motif, between residues 73 and 74. The presence of both full-size and cleaved IRBIT could also be observed in mouse cerebrum and cerebellum tissues analyzed with a specific IRBIT antibody [12]. The PEST motif is likely to be essential for the interaction with the lbd of IP_3R1, as the in vivo cleavage inside the PEST motif yielded a truncated IRBIT protein that no longer interacted with the lbd of IP_3R1. Moreover, deletion of the complete PEST motif, deletion of aa 70–73 or 82–88 or one specific point-mutation at position 73 disabled the interaction with the IP_3R. The importance of the negatively charged Asp residue at position 73 seems to be specific as mutation of a neighboring negatively charged cluster, peptide 86-DDE-88, to a positively charged cluster had no effect. Irreversible proteolytic degradation of IRBIT targeted by the PEST motif could offer the cell a mechanism to regulate IRBIT functioning.

PDZ-ligands are generally present in the very C-terminus of proteins and bind to PDZ domains. These protein–protein interaction motifs predominate in submembranous scaffolding proteins [22–24]. Using pull-down techniques, we showed that the PDZ-ligand of IRBIT mediates an IP_3-insensitive interaction with the lbd of IP_3R1. This interaction was synergistic with the IP_3-sensitive binding via the PEST motif, as a deletion mutant of the PDZ-ligand, IRBIT[ΔPDZ], showed much weaker binding than the wild-type IRBIT. However, this PDZ-ligand-mediated interaction is still likely to be dependent on the presence of the PEST motif as the PDZ-ligand of IRBIT[ΔPEST] alone did not enable an in vitro interaction with the lbd of IP_3R1 nor an in vivo reticular localization (data not shown). We do not exclude that the PDZ-ligand might also target IRBIT to other proteins than the IP_3R. This could be important for the formation of multi-protein signalling complexes containing IRBIT.

In conclusion, our study reports direct, functional effects of IRBIT on the IP_3R. We showed that IRBIT not only competed for binding of IP_3 to the lbd of IP_3R, but that it was also an attenuator of the IICR. Both IRBIT and the suppressor domain may represent different cellular protection mechanisms to avoid unwanted or exaggerated activation of the IICR. Whereas the intramolecular suppressor domain constitutes an inherent attenuator, IRBIT could operate on a subpopulation of IP_3Rs present in specific protein complexes and thereby affect more specific cell functions.

Acknowledgments

We are grateful for excellent technical assistance, especially by T. Luyten and S. Vangeel, and fruitful discussions with Ir. F. De Smet, Dr. J. Goris, and L.'tje Verbert. We also thank Dr. K. Mikoshiba (University of Tokyo, Japan) for interesting scientific discussions and for supplying the L15 cells and the p400C1 plasmid containing the cDNA of mouse IP_3R1. This work was supported by Grants G.0210.03 (to H.D.S. and J.B.P.) and G.0124.03 (to E.W.) from the Fund for Scientific Research Flanders (Belgium) and Grant GOA 2004/07 from the Concerted Actions of the K.U. Leuven (to G.C., L.M., J.B.P., and H.D.S.). We are also grateful for the support by the Interuniversity Attraction Poles Programme-Belgian Science Policy, P5/05. B.D. and N.N.K. are research assistant and postdoctoral fellow, respectively, from the Fund for Scientific Research Flanders. E.W. is part of BioMacS, the K.U. Leuven Interfacultary Centre for Biomacromolecular Structure (http://biomacs.kuleuven.be/).

References

[1] M.J. Berridge, Inositol trisphosphate and calcium signalling, Nature 361 (1993) 315–325.
[2] T. Furuichi, K. Mikoshiba, Inositol 1,4,5-trisphosphate receptor-mediated Ca^{2+} signaling in the brain, J. Neurochem. 64 (1995) 953–960.
[3] T.C. Südhof, C.L. Newton, B.T. Archer, Y.A. Ushkaryov, G.A. Mignery, Structure of a novel $InsP_3$ receptor, EMBO J. 10 (1991) 3199–3206.
[4] F. Yoshikawa, M. Morita, T. Monkawa, T. Michikawa, T. Furuichi, K. Mikoshiba, Mutational analysis of the ligand binding site of the inositol 1,4,5-trisphosphate receptor, J. Biol. Chem. 271 (1996) 18277–18284.
[5] M.J. Berridge, M.D. Bootman, P. Lipp, Calcium—a life and death signal, Nature 395 (1998) 645–648.
[6] M.J. Berridge, P. Lipp, M.D. Bootman, The versatility and universality of calcium signalling, Nat. Rev. Mol. Cell Biol. 1 (2000) 11–21.
[7] S. Patel, S.K. Joseph, A.P. Thomas, Molecular properties of inositol 1,4,5-trisphosphate receptors, Cell Calcium 25 (1999) 247–264.
[8] L. Glouchankova, U.M. Krishna, B.V. Potter, J.R. Falck, I. Bezprozvanny, Association of the inositol (1,4,5)-trisphosphate receptor ligand binding site with phosphatidylinositol (4,5)-bisphosphate and adenophostin A, Mol. Cell Biol. Res. Commun. 3 (2000) 153–158.
[9] E.C. Thrower, R.E. Hagar, B.E. Ehrlich, Regulation of $Ins(1,4,5)P_3$ receptor isoforms by endogenous modulators, Trends Pharmacol. Sci. 22 (2001) 580–586.
[10] G. Bultynck, K. Szlufcik, N. Nadif Kasri, Z. Assefa, G. Callewaert, L. Missiaen, J.B. Parys, H. De Smedt, Thimerosal stimulates Ca^{2+} flux through inositol 1,4,5-trisphosphate receptor type 1, but not type 3, via modulation of an isoform-specific Ca^{2+}-dependent intramolecular interaction, Biochem. J. 381 (2004) 87–96.
[11] I. Bezprozvanny, The inositol 1,4,5-trisphosphate receptors, Cell Calcium 38 (2005) 261–272.

[12] H. Ando, A. Mizutani, T. Matsu-ura, K. Mikoshiba, IRBIT, a novel inositol 1,4,5-trisphosphate (IP_3) receptor-binding protein, is released from the IP_3 receptor upon IP_3 binding to the receptor, J. Biol. Chem. 278 (2003) 10602–10612.

[13] J.W. Dekker, S. Budhia, N.Z. Angel, B.J. Cooper, G.J. Clark, D.N. Hart, M. Kato, Identification of an *S*-adenosylhomocysteine hydrolase-like transcript induced during dendritic cell differentiation, Immunogenetics 53 (2002) 993–1001.

[14] L. Missiaen, H. De Smedt, J.B. Parys, M. Oike, R. Casteels, Kinetics of empty store-activated Ca^{2+} influx in HeLa cells, J. Biol. Chem. 269 (1994) 5817–5823.

[15] N. Nadif Kasri, G. Bultynck, J. Smyth, K. Szlufcik, J.B. Parys, G. Callewaert, L. Missiaen, R.A. Fissore, K. Mikoshiba, H. De Smedt, The N-terminal Ca^{2+}-independent calmodulin-binding site on the inositol 1,4,5-trisphosphate receptor is responsible for calmodulin inhibition, even though this inhibition requires Ca^{2+}, Mol. Pharmacol. 66 (2004) 276–284.

[16] J.J. Mackrill, R.A. Wilcox, A. Miyawaki, K. Mikoshiba, S.R. Nahorski, R.A. Challiss, Stable overexpression of the type-1 inositol 1,4,5-trisphosphate receptor in L fibroblasts: subcellular distribution and functional consequences, Biochem. J. 318 (1996) 871–878.

[17] I. Sienaert, L. Missiaen, H. De Smedt, J.B. Parys, H. Sipma, R. Casteels, Molecular and functional evidence for multiple Ca^{2+}-binding domains in the type 1 inositol 1,4,5-trisphosphate receptor, J. Biol. Chem. 272 (1997) 25899–25906.

[18] T. Vantus, D. Vertommen, X. Saelens, A. Rykx, L. De Kimpe, S. Vancauwenbergh, S. Mikhalap, E. Waelkens, G. Keri, T. Seufferlein, P. Vandenabeele, M.H. Rider, J.R. Vandenheede, J. Van Lint, Doxorubicin-induced activation of protein kinase D1 through caspase-mediated proteolytic cleavage: identification of two cleavage sites by microsequencing, Cell. Signal. 16 (2004) 703–709.

[19] H. Sipma, P. De Smet, I. Sienaert, S. Vanlingen, L. Missiaen, J.B. Parys, H. De Smedt, Modulation of inositol 1,4,5-trisphosphate binding to the recombinant ligand-binding site of the type-1 inositol 1,4,5-trisphosphate receptor by Ca^{2+} and calmodulin, J. Biol. Chem. 274 (1999) 12157–12162.

[20] P.F. Worley, J.M. Baraban, S. Supattapone, V.S. Wilson, S.H. Snyder, Characterization of inositol trisphosphate receptor binding in brain. Regulation by pH and calcium, J. Biol. Chem. 262 (1987) 12132–12136.

[21] M. Rechsteiner, S.W. Rogers, PEST sequences and regulation by proteolysis, Trends Biochem. Sci. 21 (1996) 267–271.

[22] A.S. Fanning, J.M. Anderson, Protein modules as organizers of membrane structure, Curr. Opin. Cell Biol. 11 (1999) 432–439.

[23] K. Bruckner, J. Pablo Labrador, P. Scheiffele, A. Herb, P.H. Seeburg, R. Klein, EphrinB ligands recruit GRIP family PDZ adaptor proteins into raft membrane microdomains, Neuron 22 (1999) 511–524.

[24] M.H. Roh, B. Margolis, Composition and function of PDZ protein complexes during cell polarization, Am. J. Physiol. Renal Physiol. 285 (2003) F377–F387.